AIP | Applied Physics Letters

Vertical cavity surface emitting lasers utilizing native oxide mirrors and buried tunnel contact junctions

J. J. Wierer, P. W. Evans, N. Holonyak Jr., and D. A. Kellogg

Citation: Applied Physics Letters **72**, 2742 (1998); doi: 10.1063/1.121445
View online: http://dx.doi.org/10.1063/1.121445
View Table of Contents: http://scitation.aip.org/content/aip/journal/apl/72/21?ver=pdfcov
Published by the AIP Publishing

Articles you may be interested in

Precise control of 1.55 μm vertical-cavity surface-emitting laser structure with InAlGaAs/InAlAs Bragg reflectors by in situ growth monitoring
Appl. Phys. Lett. **75**, 1500 (1999); 10.1063/1.124735

Tunnel contact junction native-oxide aperture and mirror vertical-cavity surface-emitting lasers and resonant-cavity light-emitting diodes
Appl. Phys. Lett. **74**, 926 (1999); 10.1063/1.123452

Al x Ga 1−x As native-oxide-based distributed Bragg reflectors for vertical cavity surface emitting lasers
J. Appl. Phys. **84**, 5436 (1998); 10.1063/1.368857

Lateral electron current operation of vertical cavity surface emitting lasers with buried tunnel contact hole sources
Appl. Phys. Lett. **71**, 3468 (1997); 10.1063/1.120400

Low threshold vertical-cavity surface-emitting lasers based on high contrast distributed Bragg reflectors
Appl. Phys. Lett. **70**, 1781 (1997); 10.1063/1.118689

This article is copyrighted as indicated in the article. Reuse of AIP content is subject to the terms at: http://scitation.aip.org/termsconditions. Downloaded to IP: 35.8.11.3 On: Mon, 25 Jan 2016 14:17:42

Vertical cavity surface emitting lasers utilizing native oxide mirrors and buried tunnel contact junctions

J. J. Wierer, P. W. Evans, N. Holonyak, Jr., and D. A. Kellogg
Electrical Engineering Research Laboratory and Center for Compound Semiconductor Microelectronics, University of Illinois at Urbana-Champaign, Urbana, Illinois 61801

(Received 12 February 1998; accepted for publication 18 March 1998)

Vertical cavity surface emitting lasers (VCSELs) are demonstrated with high-index-contrast native-oxide-based (Al_xO_y) distributed Bragg reflectors (DBRs) on both sides of a ''2λ'' cavity, thus creating a compact (thin, ~2.8 μm) laser structure. Selective oxidation of high Al composition $Al_xGa_{1-x}As$ layers yields a structure with a four period upper Al_xO_y/GaAs DBR, a 5.5 period lower Al_xO_y/GaAs DBR, and a buried oxide current aperture. A reverse-biased tunnel contact junction provides hole injection via lateral electron current between the upper DBR and the oxide aperture layer. These VCSELs operate with submilliampere thresholds, high spontaneous efficiencies, and excellent polarization control. © *1998 American Institute of Physics.* [S0003-6951(98)03820-0]

The vertical cavity surface emitting laser (VCSEL)[1] offers various advantages over other light sources, including a symmetrical output beam and ease of manufacturing in the form of two-dimensional arrays. In fact it is now replacing the standard edge-emitting laser and light emitting diode (LED) in many optical data communications applications. Recent advances in VCSELs such as ultralow thresholds[2] and high efficiencies[3] owe their existence to the native oxidation of high Al composition III–V compounds.[4] This wet oxidation process can proceed laterally (along heterolayers) to create buried-native-oxide layers (apertures) that define current and confining cavities in laser structures,[5] and then was first used in VCSELs by Deppe and co-workers.[6] Further improvements may come with a reduction in cavity size, which in turn reduces the number of cavity modes. Small apertures decrease the cavity size, but at smaller diameters ($\leqslant 3$ μm) VCSEL performance degrades because of optical scattering or diffraction loss. Another method to reduce the cavity size is to decrease the effective length (optical mode length) in the vertical direction by substituting high contrast native-oxide-based Al_xO_y/GaAs distributed Bragg reflectors (DBRs) in place of the usual lower contrast AlGaAs/GaAs DBRs. Spontaneous light is used more efficiently in highly defined thin cavities[7] as demonstrated by more efficient LEDs[8] and edge-emitting lasers with high spontaneous efficiencies.[9,10] Although VCSELs with Al_xO_y/GaAs DBRs have been demonstrated previously,[11] the thick conducting layers employed have resulted in a large cavity size.

In this letter we demonstrate an alternative way to create VCSELs with compact cavity sizes. Vertical feedback between a ''2λ'' cavity (including conducting layers) is provided by a 4 period upper and a 5.5 period lower Al_xO_y/GaAs DBR, yielding a total thickness of ~2.8 μm. A buried-native-oxide aperture defines current and cavity in the lateral direction. Current is fed by two thin (λ/4 thickness) n-type conducting layers, one on the top and the other on the bottom of the cavity. On the top a reversed-biased tunnel contact junction (TJ, $p+/n+$), located between the upper DBR and oxide aperture layer, supplies holes to the p-type crystal above the active region by lateral electron currents.[12,13] Current flow beyond the active region occurs along the bottom n-type conducting layer, wrapping around the lower DBR, and exiting through the substrate (see Fig. 2 of Ref. 13). All lateral conduction is by electron current to avoid high resistance, extra voltage drop, and heating. These VCSELs display high spontaneous efficiencies, submilliampere thresholds, and excellent polarization control.

The crystal used in this work is grown by low-pressure metalorganic chemical-vapor deposition (MOCVD)[14] on (100) n-type GaAs substrates misoriented ~2° to the ⟨101⟩ with Se used as the n-type dopant and C as the p-type dopant. Crystal growth begins with a 5.5 period stack of n-type $Al_{0.98}Ga_{0.02}As$/GaAs, with buffer layers, that are each ~λ/4 thickness after oxidation. Then n-type λ/4 thickness GaAs and ~700 Å of $Al_{0.70}Ga_{0.30}As$ are grown for bottom-side lateral conduction. The unintentionally doped cavity consists of two ~400 Å $Al_{0.50}Ga_{0.50}As$ layers sandwiching ~2050 Å of GaAs with two InGaAs quantum wells (QWs) in the center. A gain peak at λ~980 nm is intended, but an extra gain peak is also present at ~950 nm. Beyond the cavity a p-type ~500 Å $Al_{0.95}Ga_{0.05}As$ confining layer, with buffer layers, is grown, and is later oxidized to form the current aperture. Next an ~λ/4 thickness p^+/n^+ GaAs tunnel junction is grown that supplies holes to the active region by lateral electron conduction. The p^+ ($p \gtrsim 10^{20}$ cm^{-3}) layer is kept thin (~75 Å) to minimize free carrier loss. Finally the structure is completed with a four-period stack of $Al_{0.98}Ga_{0.02}As$/GaAs, with buffer layers, which are also ~λ/4 thickness after oxidation.

The VCSELs are fabricated by first defining an ~15 μm diameter disk with photoresist. Then selective wet etching is used to etch through the entire upper DBR, stopping on the tunnel junction. This forms a mesa (a tapered disk) out of the upper DBR that is undercut below the mask to a diameter of ~10 μm at the top and ~15 μm at the bottom. Next, using photolithography and wet etching (H_2SO_4:H_2O_2:H_2O 1:8:40), we form an ~48 μm wide trench (~20 μm away from the etched disk), thus exposing the lower DBR for oxidation. An ~24 μm diameter protective disk of photoresist is then centered on the original ~15 μm etched disk, and the

This article is copyrighted as indicated in the article. Reuse of AIP content is subject to the terms at: http://scitation.aip.org/termsconditions. Downloaded to IP: 35.8.11.3 On: Mon, 25 Jan 2016 14:17:42

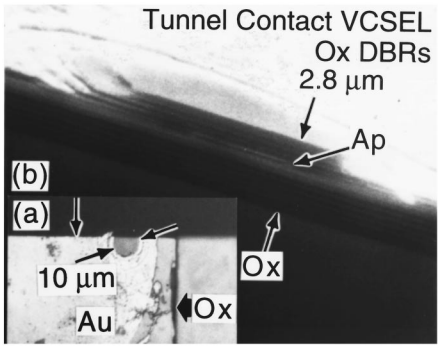

FIG. 1. (a) Optical microscope image (top view) of a cleaved sample and (b) scanning electron microscope (SEM) image (cross section) of a tunnel contact VCSEL with native-oxide-based (top and bottom) distributed Bragg reflectors (DBRs). Oxidation of the lower DBR proceeds laterally from the trench (stubby arrow labeled ''Ox'') $\sim 40\ \mu$m underneath the structure to the unmarked downward vertical arrow in (a). The top of the upper DBR is $\sim 10\ \mu$m in diameter. The SEM image (b) shows that the upper DBR is completely oxidized, and that an oxide aperture (''Ap'') is formed underneath.

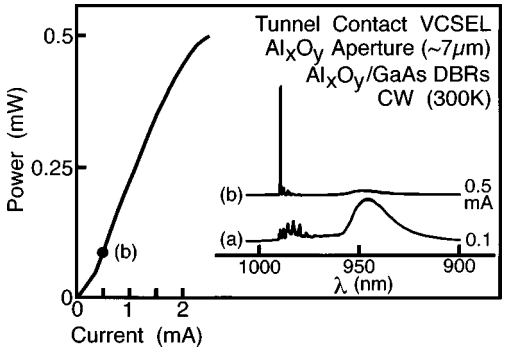

FIG. 2. The light vs current ($L-I$) characteristic and spectral curves of a tunnel contact VCSEL with native-oxide-based DBRs. The spontaneous efficiency is $\sim 11.5\%$. Threshold current is $I_{th} \sim 350\ \mu$A, and the external differential quantum efficiency $\eta \sim 20\%$. At 0.1 mA ringing also occurs at the resonant wavelength with extra recombination radiation at 950 nm. At 0.5 mA one mode is present (990 nm), with single mode operation persisting to $3 \times I_{th}$.

sample is wet etched again so that the $Al_{0.95}Ga_{0.05}As$ aperture layer is exposed. This creates an annulus mesa around the upper DBR that allows metal contacting to the tunnel junction. Finally the sample is placed in a ''wet'' oxidation open tube furnace (H_2O in a N_2 carrier gas) for 55 min at 430 °C to oxidize the high Al composition layers.[4]

Figure 1 shows (a) a top-view optical microscope image of a cleaved sample of the native-oxide-based DBR tunnel contact VCSEL and (b) the corresponding scanning electron microscope (SEM) image (cross section). Although the device is completed [note the ''Au'' contact pad in (a)], the cross section [Figs. 1(a) and 1(b)] is also convenient in illustrating the fabrication process just through oxidation. The lateral oxidation of the lower DBR [Fig. 1(a)] proceeds from the trench (stubby arrow marked ''Ox'') for a distance of $\sim 40\ \mu$m up to the unmarked downward vertical arrow. The lower DBR oxidizes beyond the upper DBR and the contact annulus. In fact it overshoots too far, which only adds resistance. The pair of arrows in Fig. 1(a) marks the diameter of the top layers of the upper DBR ($\sim 10\ \mu$m) after etching. The SEM image (b) shows that the aperture layer (arrow marked ''Ap'') oxidizes underneath the upper DBR from the $\sim 24\ \mu$m diameter disk edge, resulting in an aperture diameter of $\sim 7\ \mu$m. The upper DBR is completely oxidized, completing the $\sim 2.8\ \mu$m thick structure.

After the oxidation process, ~ 1500 Å of SiO_2 is deposited on the crystal everywhere except on the upper DBR and the annulus contact region. This prevents shorting in subsequent metallizations. Ti/Au is evaporated to make metal contact to the tunnel junction, leaving an $\sim 15\ \mu$m opening centered on the upper DBR. The crystal is then lapped and polished to $\sim 125\ \mu$m thickness, and Ge/Au is evaporated and alloyed to the substrate side of the sample. All measurements are taken at room temperature (300 K) under continuous wave (cw) conditions on diodes mounted epitaxial layer side upward on In-coated copper heat sinks. Power measurements ($L-I$) are performed in an integrating sphere.

The light versus current ($L-I$) and spectra (inset) of a native-oxide-based DBR tunnel contact VCSEL are shown in Fig. 2. Some of the VCSELs tested have spontaneous efficiencies as high as 14%. This agrees with data on earlier devices[9,10,13] having thin highly defined cavities, and is a result of the more efficient use of the spontaneous emission.[7] The threshold current (I_{th}) of the VCSEL of Fig. 2 is $\sim 350\ \mu$A, and all the devices tested have thresholds between 250 and 500 μA. Beyond threshold the differential quantum efficiency of the VCSEL is $\eta \sim 20\%$, which is low but comparable to other VCSELs with similar mirror sets.[11] Decreasing the losses (mirror, free carrier) should increase the efficiency. At 0.1 mA spectral ringing occurs at the cavity resonance, but also an extra gain peak is evident at 950 nm. This is wasted recombination that increases the threshold. At 0.5 mA one mode is present ($\lambda \sim 990$ nm), and single mode operation persists until $3 \times I_{th}$. The current versus voltage characteristic (data not shown) turns on at 1.2 V, and threshold occurs at 2.2 V. The series resistance is $R_s \sim 800\ \Omega$ at I_{th} and $360\ \Omega$ at $10 \times I_{th}$. The series resistance may be reduced by improved contacting of the top side of the crystal and by reducing the oxidation length of the lower DBR (the ''overshoot'').

Figure 3 shows near-field (NF) and far-field (FF) data for the VCSEL of Fig. 2. The NF data on the left show the width of the beam measured parallel to the oxidation trench

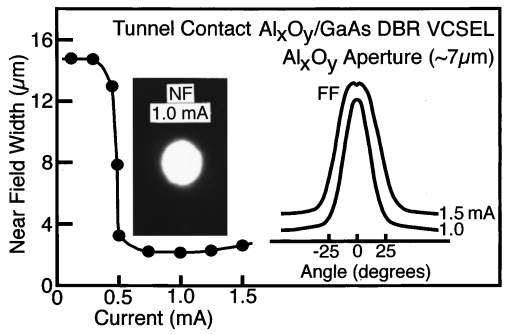

FIG. 3. Near-field (NF) and far-field (FF) data (left to right) for the tunnel contact VCSEL with the native-oxide-based DBRs of Fig. 2. The NF full width at half-maximum (FWHM) measured parallel to the device oxidation trench is as wide as the upper metal contact opening until spectral narrowing occurs at laser threshold ($I = I_{th}$). The minimum NF width ($I > I_{th}$) is $\sim 2.2\ \mu$m. The NF image at 1.0 mA exhibits a slightly oval shape. The FF plot measured parallel to the trench is single lobed at 1.0 mA, and at 1.5 mA produces side lobes.

This article is copyrighted as indicated in the article. Reuse of AIP content is subject to the terms at: http://scitation.aip.org/termsconditions. Downloaded to IP: 35.8.11.3 On: Mon, 25 Jan 2016 14:17:42

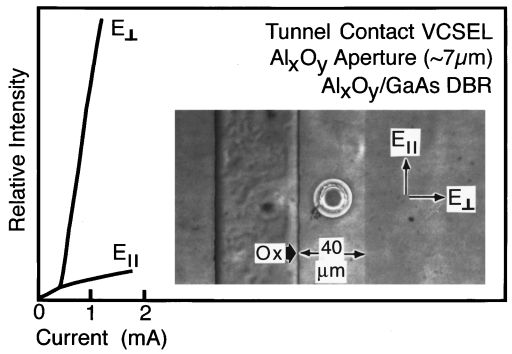

FIG. 4. Polarized light vs current ($L-I$) characteristic for the tunnel contact VCSEL with the native-oxide-based DBRs of Figs. 2 and 3. The inset (for reference) is an unmetallized device, and defines $E_\parallel$ and $E_\perp$ with respect to the trench. The laser output is polarized in the $E_\perp$ direction. The VCSEL polarization is maintained up to the maximum output power of the device.

of the device. Below threshold the NF full width at half-maximum (FWHM) is as wide as the Ti/Au metal contact opening. Narrowing occurs at threshold, and the output is single lobed with a minimum width of $\sim 2.2\ \mu$m at 0.7 mA. Widening of the NF occurs with increased excitation. The inset shows the NF image of this device at 1.0 mA, with the trench (not visible) extending vertically in this view. A single spot is shown that is slightly oval, wider in the vertical direction (parallel to the trench). The inset on the far right shows the FF of the device, also measured parallel to the trench direction. The FF pattern is single lobed at 1.0 mA (13°) and remains fixed up to $3\times I_{\text{th}}$. Beyond this current side lobes appear, shown here at 1.5 mA (17.5°). Measuring perpendicular to the trench gives similar but wider FF patterns (14° at 1.0 mA and 18° at 1.5 mA), confirming the slightly asymmetric output of the device.

The output polarization of the VCSEL of Figs. 2 and 3 is shown in Fig. 4. The inset shows (nonmetallized VCSEL) $E_\parallel$ and $E_\perp$ defined with respect to the oxidation trench. The $L-I$ curves show that the laser output is polarized in the $E_\perp$ direction, with the $E_\parallel$ direction producing only spontaneous light. All of the VCSELs exhibit this behavior. The polarized output persists up to the maximum output power of the device. Polarization control has been achieved with oval-apertured VCSELs previously,[3] but with the polarization aligned with the longer axis of the aperture. Here the opposite occurs, which suggests that another feature determines the polarization. The oxidation of the lower DBR from a trench produces a natural asymmetry in the device. The oxidation process proceeds from the trench tapering (shrinking) slightly, thus creating a slight detuning of the lower DBR and cavity horizontally away from the trench. Also, the oxidation undoubtedly induces stress. Additionally, current on the bottom side of the VCSEL flows in the same direction that the light is polarized, perpendicular to the trench, and may influence the polarization. One or all of these contribute to the polarization control.

Finally, compact VCSELs (total thickness $\sim 2.8\ \mu$m) have been achieved with the use of native-oxide-based DBRs, buried oxide apertures, and thin n-type GaAs lateral current-feed layers augmented with a tunnel contact junction on the p side to supply hole injection. These devices display the high spontaneous efficiencies characteristic of other thin cavity devices, and exhibit low current thresholds despite the nonideal gain profile. Also, the form of the device leads to complete polarization control. Since the lateral conducting layers used in these VCSELs are thin, more compact structures can be achieved in further work by resorting to ''one-λ'' cavities to make even more efficient use of the spontaneous emission ($I<I_{\text{th}}$).

The authors are grateful to R. T. Gladin and B. Payne for assistance in manuscript preparation. Also, one of them (N.H.) wishes to thank the Sony Corporation for the support of the John Bardeen Chair. This work has been supported by the Army Research Office, Contract DAAH 04-96-1-0333 (J. Zavada) and the National Science Foundation, Grant No. SBC UTA-97-0080.

[1] K. Iga, F. Koyama, and S. Kinoshita, IEEE J. Quantum Electron. **24**, 1845 (1988).
[2] G. M. Yang, M. H. MacDougal, and P. D. Dapkus, Electron. Lett. **31**, 886 (1995).
[3] B. Weigl, M. Grabherr, C. Jung, R. Jäger, G. Reimer, R. Michalzik, D. Sowada, and K. J. Ebeling, IEEE J. Sel. Top. Quantum Electron. **3**, 409 (1997).
[4] J. M. Dallesasse, N. Holonyak, Jr., A. R. Sugg, T. A. Richard, and N. El-Zein, Appl. Phys. Lett. **57**, 2844 (1990).
[5] S. A. Maranowski, A. R. Sugg, E. I. Chen, and N. Holonyak, Jr., Appl. Phys. Lett. **63**, 1660 (1993).
[6] D. L. Huffaker, D. G. Deppe, K. Kumar, and T. J. Rogers, Appl. Phys. Lett. **65**, 97 (1994).
[7] T. J. Rodgers, D. G. Deppe, and B. G. Streetman, Appl. Phys. Lett. **57**, 1858 (1990).
[8] D. L. Huffaker, C. C. Lin, J. Shin, and D. G. Deppe, Appl. Phys. Lett. **66**, 3096 (1995).
[9] P. W. Evans, N. Holonyak, Jr., S. A. Maranowski, M. J. Ries, and E. I. Chen, Appl. Phys. Lett. **67**, 3168 (1995).
[10] J. J. Wierer, P. W. Evans, and N. Holonyak, Jr., Appl. Phys. Lett. **72**, 797 (1998).
[11] M. H. MacDougal, G. M. Yang, A. E. Bond, C. Lin, D. Tishinin, and P. D. Dapkus, IEEE Photonics Technol. Lett. **8**, 310 (1996).
[12] J. J. Wierer, P. W. Evans, and N. Holonyak, Jr., Appl. Phys. Lett. **71**, 2286 (1997).
[13] J. J. Wierer, P. W. Evans, N. Holonyak, Jr., and D. A. Kellogg, Appl. Phys. Lett. **71**, 3468 (1997).
[14] R. D. Dupuis, L. Moudy, and P. D. Dapkus, in *Proceedings of the International Symposium on GaAs and Related Compounds*, edited by C. M. Wolfe (Institute of Physics, London, 1979), pp. 1–9; see also, M. J. Ludowise, J. Appl. Phys. **58**, R31 (1985).

This article is copyrighted as indicated in the article. Reuse of AIP content is subject to the terms at: http://scitation.aip.org/termsconditions. Downloaded to IP: 35.8.11.3 On: Mon, 25 Jan 2016 14:17:42